International Journal of Offshore and Coastal Engineering
Vol.1 | No. 2 | pp. 100 – 107 | November 2017
e-ISSN: 2580-0914

Submitted: July 11, 2017 | Revised: August 15, 2017 | Accepted: October 17, 2017

Analitical Study of Vertical and Lateral Buckling on Pipeline Using Hobbs Method

Yoyok S Hadiwidodo[a,*], Muhammad M Romadhoni[b], and Herman Pratikno[c]

[a)] Undergraduate Student, Department of Ocean Engineering, Institut Teknologi Sepuluh Nopember, Surabaya, Indonesia
[b)] Lecturer, Department of Ocean Engineering, Institut Teknologi Sepuluh Nopember, Surabaya, Indonesia
[c)] Lecturer, Department of Ocean Engineering, Institut Teknologi Sepuluh Nopember, Surabaya, Indonesia
*Corresponding author: yoyoksetyo@oe.its.ac.id

ABSTRACT

During its operation, the pipeline will receive loads of internal pressure and thermal loads of fluid flowed until the pipes have both vertical and lateral buckling. Numerical analysis of vertical and lateral buckling Hobbs this method on a high friction coefficient and the coefficient of friction ($0.3 \leq \varphi \leq 0.7$) as well as the length of buckling as many as 20 variants were then performed comparisons, as well as axial tension comparison with DnV RP L110. So we get the relationship of temperature increase with the length and amplitude buckling. The data which is used is the gas pipeline Labuhan Maringgai-Muara Bekasi PT. Perusahaan Gas Negara (Persero) Tbk., Including the outer diameter of the pipe = 0.8128 m, plate thickness = 0.015875 m, thermal linear expansion coefficient = 11 x 10-6 m / ^oC, etc. So the higher coefficient of friction, temperature rise of 13.4%, 13.4% reduced buckling length, and axial tension increased to 12.95%. For the comparisons, the coefficient of friction does not affect the length of buckling on the vertical buckling. Comparison with DnV RP F110, increased coefficient of friction will increase the voltage axial (S_{eff}) of 0.00024% and up 13.4% axial stress (P_0) Hobbs.

Keywords: *Buckling, DnV RP F110, Friction Coefficient, Hobbs Method, Pipeline*

1. INTRODUCTION

The process of taking oil and gas offshore using pipeline has many advantages, but the cost of failure that occurred on the pipeline structure is also very high. One of the failures that often occur is buckling. This failure is bending deformation that occurs either at the pipe wall and across all parts of the pipe. If the soil prisoners style is not big enough to withstand the force impulse that caused the pipe so the pipe will form the curve as a result of deformation due to thermal expansion.

During pipeline operation, the pipeline will receive loads of internal pressure and thermal loads of fluid or gas delivered by the pipeline. Expenses incurred by a pipeline system will cause the pipe to be in a state of tension. As is known, the pipe material is also resistant to stress and ultimately will be fail.

2. DESCRIPTION OF RESEARCH

2.1 Buckling

There are two types of buckling, ie local and global buckling buckling.

a. Local buckling: plastic deformation on the pipe, which is caused by external pressure or due to external pressure combined with bending. The occurrence of collapse (dents) can continue to propagate along the pipeline. This is called propagating buckling.

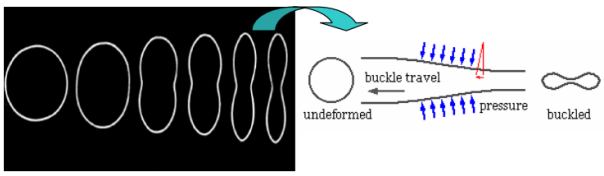

Figure 1. Collapse and propagation buckling [12].

b. Global buckling is excessive deflection that occurred on the pipeline. There are three types of global buckling, namely: Upheaval buckling, lateral buckling, and downward on free span.

Figure 2. Global buckling (vertical buckling) [9].

A pipe otherwise damaged or fail if the force occurs in the pipeline exceeds the allowable limit of the material.

2.2 Pure Bending Theory and Euler Equations

In this theory, the force acting on a beam is assumed to be in steady is only on a straight beam and is given to the beam without shock or collision.

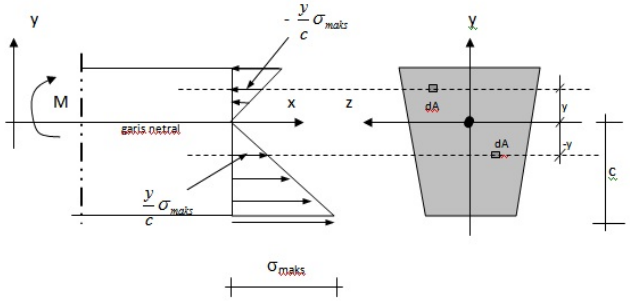

Figure 3. Pure bending of Beam [8].

Based on the image above, the segment beam in equilibrium, then $\Sigma F_x = 0$. Thus,

$$\sigma_{max} = \frac{Mc}{I} \tag{1}$$

And the normal voltage is,

$$\sigma_{max} = -\frac{My}{I} \tag{2}$$

According to Euler, for columns hinged at both ends (K = 1) and $I = Ar^2$, then the critical stress is,

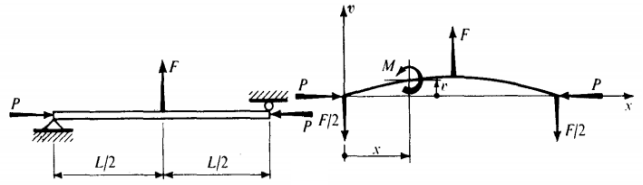

Figure 4. The Free body diagram for the column is deflected [8].

$$P_{cr} = \frac{\pi^2 EI}{(KL)^2} = \frac{\pi^2 EAr^2}{L^2} \tag{3}$$

or

$$\sigma_{cr} = \frac{P_{cr}}{A} = \frac{\pi^2 E}{(L/r)^2} \tag{4}$$

2.3 Hobbs Buckling Theory

The force (P_0) that occurs due to temperature change can be expressed as follows bellow

$$P_0 = EA\alpha T \tag{5}$$

a. Vertical Buckling

Vertical buckling analysis performed on a high friction coefficient and the actual friction coefficient ($0.3 \leq \varphi \leq 0.7$). Bending moment on the lift-off point assumed to be zero and on small slope. Here is an overview of vertical buckling axial stress distribution on the pipeline,

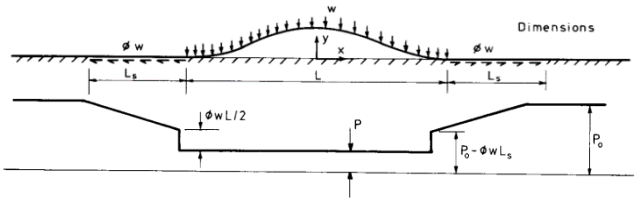

Figure 5. The presures distribution on vertical buckling [6].

The condition of distribution severed in each end are combined with the reaction that occurred vertically centered. Thus, based on the diagram above, the vertical buckling analysis begins with determining the minimum buckling length that is,

$$L_{min} = \left(\frac{1{,}6856\ x\ 10^6 (EI)^3}{w^2 AE}\right)^{0{,}125} \tag{6}$$

By varying L of 20 with a range 0,1L-3L, then obtained,

$$P = 80{,}76EI/L^2 \tag{7}$$

Use these results, it can be determined the axial pressure (P_0),

$$P_0 = P + \frac{wL}{EI}[1{,}597\ x\ 10^{-5} EA\phi wL^5 - 0{,}25(\phi EI)^2]^{\frac{1}{2}} \tag{8}$$

use these results, will obtain the value of the temperature (T) using the formula and the maximum buckling amplitude (y) which are accured with the following equation,,

$$y_{max} = 2{,}408\ x\ 10^{-3}\ \frac{wL^4}{EI} \tag{9}$$

b. Lateral Buckling

Lateral buckling shape resembles a vertical mode 1 buckling so that it can be assumed that the lateral friction coefficient equal to the coefficient of friction to the movement in the axial length of the pipe (L_s) which is nearby. Here are some pictures form that occurs in the lateral buckling,

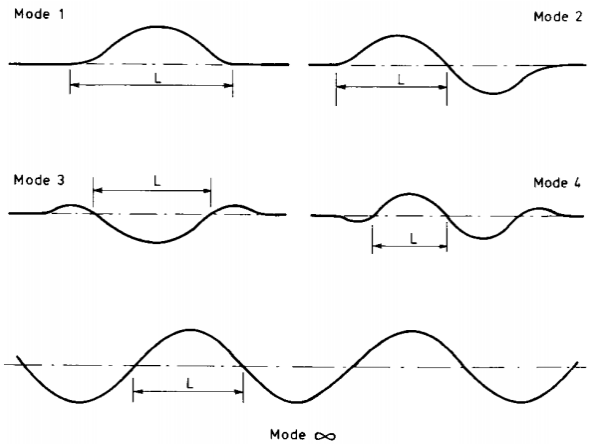

Figure 6. The lateral buckling shape [6].

But for Mode 1 requires a centrally lateral pressure with $\phi wL/2$ at each end of the buckling. In addition, the friction coefficient of lateral buckling is assumed to move everywhere.

Lateral buckling analysis performed on infinite mode and mode 1-4 on each coefficient ($0.3 \leq \varphi \leq 0.7$). In the infinite mode, to determine the minimum length of buckling, can be done by the following equation,

$$L_{min} = \left(\frac{9{,}0474\ x\ 10^5 (EI)^3}{(\phi w)^2 AE}\right)^{0{,}125} \quad (10)$$

With 20 variations 0,5L-1,5L, can obtain the pressure (P), using the following equation,

$$P = 4\pi^2 EI/L^2 \quad (11)$$

And the axial pressure (P_0),

$$P_0 = P + 1{,}4545\ x\ 10^{-5} AE \left(\frac{\phi w}{EI}\right)^2 L^6 \quad (12)$$

So, it can be known of the maximum buckling amplitude (y) as the following,

$$y_{max} = 4{,}4495\ x\ 10^{-3} \frac{\phi w}{EI} L^4 \quad (13)$$

As well as the temperature (T), which occurs in the equation.

In this case, Martinet and Kerr in Hobbs (1981) has concluded the equation to determine the lateral buckling modes 1-4 and infinite use the following constants,

Table 1. The coefficient for each mode of *lateral buckling* [6].

Mode	Constants			
	k_1	k_2	k_3	k_4
1	80,76	6,391 x 10^{-5}	0,5	2,407 x 10^{-3}
2	$4\pi^2$	1,743 x 10^{-4}	1	5,532 x 10^{-3}
3	34,06	1,668 x 10^{-4}	1,294	1,032 x 10^{-2}
4	28,2	2,144 x 10^{-4}	1,608	1.047 x 10^{-2}
∞	$4\pi^2$	1,4545 x 10^{-5}	Eqn. 12	4,4495 x 10^{-3}

Thus, the pressure that occurs as follows,

$$P = k_1 EI/L^2 \quad (14)$$

Then the axial pressure (P_0),

$$P_0 = P + k_3 \phi wL \left[\left(1 + k_2 \frac{AE\phi wL}{(EI)^2}\right)^{1/2} - 1\right] \quad (15)$$

And the maximum buckling amplitude (y) as following bellow,

$$y_{max} = k_4 \frac{\phi w}{EI} L^4 \quad (16)$$

2.4 Buckling Theory by DNV RP F110

Based on DNV-RP-F110 explained that there are two causes of global buckling, global buckling which occurs as a result of trawl and caused by imperfections.

a. Vertical Buckling Analysis

As the lateral buckling Hobbs, following the analysis of a linear corelation to the prop model:

$$S_{eff} = (R_{max} + w_p + k_2 w_0) \sqrt{\frac{EI}{{k_1}^2 \delta w_o}} \quad (17)$$

Where R_{max} is the total resistance and w_0 is the weight of the pipe during installation and w_p is the weight of the

pipes during the operation. δ is (prop) imperfection, EI is bending stiffness and k_1 = 2 and k_2 = 11 are constants determined from the results of Finite Element to form prop scenario.

The difference with the Hobbs method that in this method the soil resistance to vertical mode is assumed to be along the buckling happens.

b. Lateral Buckling Analysis

Global buckling which are caused by these imperfections using a basic capacity Hobbs infinite mode. So, to determine the minimum buckling length (L) as follows,

$$L = \left[\frac{(EI)^3}{(f_L^{LB})^2\, E\, A_s}\right]^{0,125} \quad (18)$$

and with 20 variations 0,5L-1,5L, effectively infinite pressure obtained by the following equation,,

$$S\infty = 2{,}29\frac{EI}{L^2} \quad (19)$$

3. MATERIALS AND METHODS

The analysis process is done numerically to determine the friction coefficient corelation against buckling length changes (L) with the buckling amplitude (y) and temperature (T). Comparing the results of vertical and lateral buckling. Comparing the results between Hobbs method with DNV.

3.1 Data Collection

The data required during operation including the data pipeline owned by PT. Perusahaan Gas Negara (Persero) Tbk. That is on the gas pipeline of Labuhan Maringgai-Muara Bekasi. These data include:

- Pipeline properties,
- Coating data, and
- Concrete data.

3.2 Analysis Using Hobbs Method

On the vertical buckling, processing the data using the method of Hobbs performed at a high friction coefficient, will be obtained Buckling Length (L) of 20 values (the value range 0,1L-3L), pressure (P_0), Varian temperature (T), and amplitude (Y). Then, the data processing method Hobbs with actual friction coefficient, the friction coefficient range ($0.3 \leq \varphi \leq 0.7$) will be obtained Buckling Length (L) of 20 values (the value range 0,1L-3L), Pressure (P_0), Varian temperature (T), and amplitude (y). Furthermore, the data processing method to form an infinite Hobbs on any range of coefficient of friction ($0.3 \leq \varphi \leq 0.7$), will be obtained Buckling Length (L) of 20 values (the value range 0,5L-1,5L), pressure (P_0), Varian temperature (T), and amplitude (y).

Further to lateral buckling, the data processing will be carried out using the method of Hobbs to form 1-4 in each range coefficient of friction ($0.3 \leq \varphi \leq 0.7$), will be obtained of Buckling Length (L) of 20 values (the range of values 0,5L-2L), pressure (P_0), Varian temperature (T), and amplitude (y).

3.3 Analysis Using DNV RP F110

For vertical buckling count of Axial Stress Effectively (P_0) experienced by the pipeline. Likewise, lateral buckling calculation Axial Stress Effectively (P_0) that occurs in the pipeline.

4. RESULTS AND DISCUSSION

4.1 Data Analysis

The analysis process using pipeline offshore data of PT. Perusahaan Gas Negara (Persero) Tbk. where those pipeline are gas pipeline networks of Labuhan Maringgai-Muara Bekasi. Pipelines are transmission pipelines that deliver gas from Sumatra Island to Java through the Straits of Sunda.

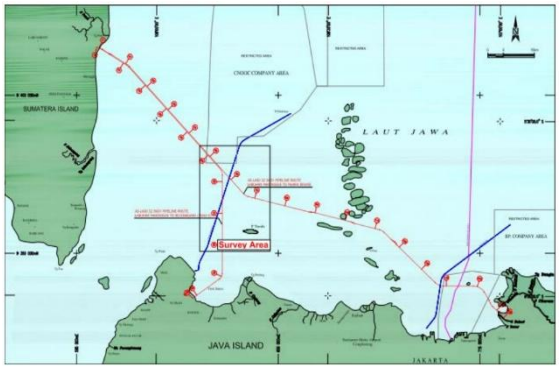

Gambar 7. The location of offshore pipeline network of PT. Perusahaan Gas Negara (Persero) Tbk.

Based on data from the current pipeline operations include outer diameter, plate thickness, density pipe, coatings of data, and data is concrete, it is known that other values such properties of pipeline:

- Cross Section Area (A) = 0,0397 m^2
- Massa per unit length (W) = 8077,7057 N/m
- Inertia moment (I) = 0,0032 m^4
- Coefficient of Linear Thermal Expansion (α) = 0,000011 $m/^oC$
- Yield Pressure of Pipeline (E) = 2,07 x 10^{11} Pa

4.2 Vertical Buckling Analysis Using Hobbs Method

Based on the equation 6, are gotten a score of L_{min} 73.76 m by 20 variations that is 0,1L-3L. So that the friction coefficient is very high, we obtained two graphs as follows,

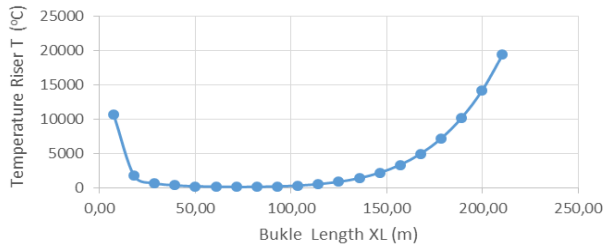

Figure 8. The Graph corelation of buckling length (L) and temperature (T).

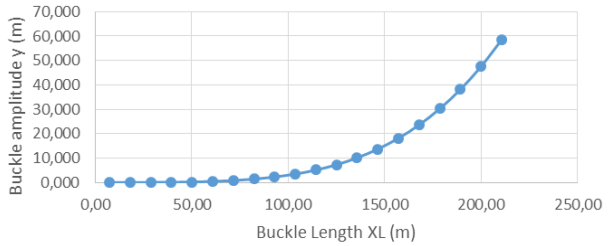

Figure 9. Graph corelation of buckling length (L) with the buckling amplitude (y).

While the actual friction coefficient are ($0.3 \leq \varphi \leq 0.7$) obtained graph as follows,

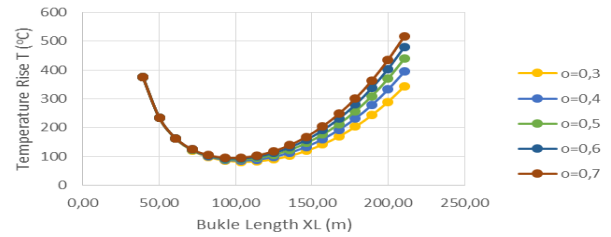

Figure 10. Graph correlation of buckling length (L) to temperature (T).

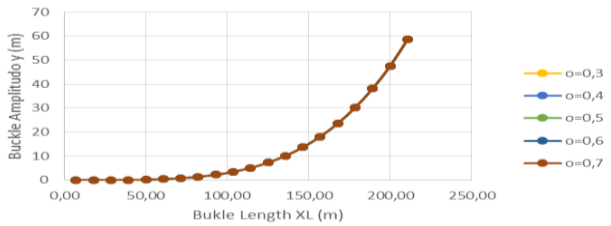

Figure 11. Graph correlation of buckling length (L) to buckling amplitude (y).

4.3 Lateral Buckling Analysis Using Hobbs Method

It's contrast to vertical buckling, to determine the minimum buckling length (L_{min}) is performed at each coefficient of friction. So we get the value L_{min} as follows,

Table 2. Values L_{min} at each coefficient of friction

ϕ	L_{min}
0,30	111,33 m
0,40	103,61 m
0,50	97,98 m
0,60	93,62 m
0,70	90,08 m

In the infinite mode, the analysis process uses some constants, $k_1 = 4\pi^2$, $k_2 = 1{,}4545 \times 10^{-5}$, and $k_3 =$ (equation 28), $k_4 = 4{,}4495 \times 10^{-3}$.. So we get some of the following graph,

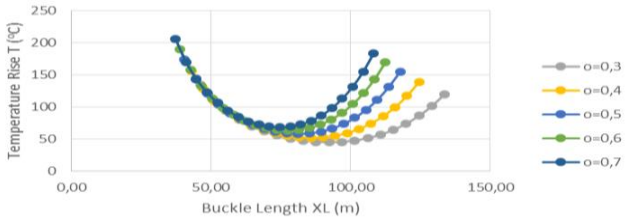

Figure 12. Graph corelation of buckling length (L) to changes in temperature (T) of infinite mode.

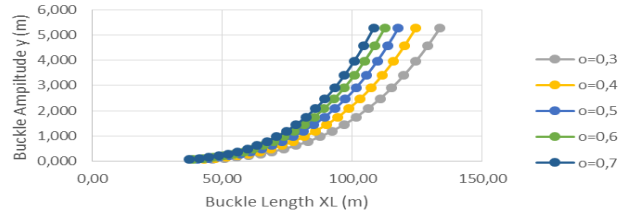

Figure 13. Graph correlation of buckling length (L) to buckling ampitude (ŷ) of infinite mode.

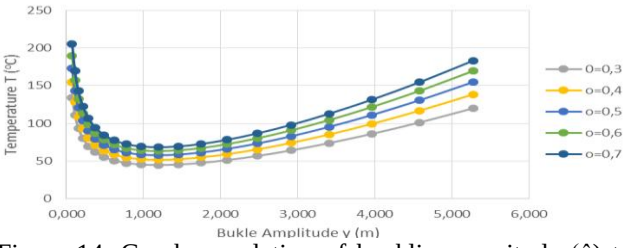

Figure 14. Graph correlation of buckling ampitude (ŷ) to changes in temperature (T) of infinite mode.

In mode 1, the analysis process using some constants, $k_1 = 80{,}76$, $k_2 = 6{,}391 \times 10^{-5}$, and $k_3 = 0{,}5$, $k_4 = 2{,}407 \times 10^{-3}$. So we get some of the following graph:

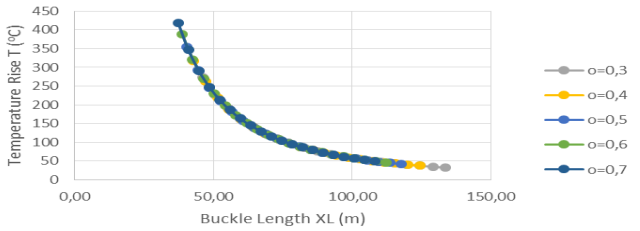

Figure 15. Graph correlation of buckling length (L) to changes in temperature (T) mode 1.

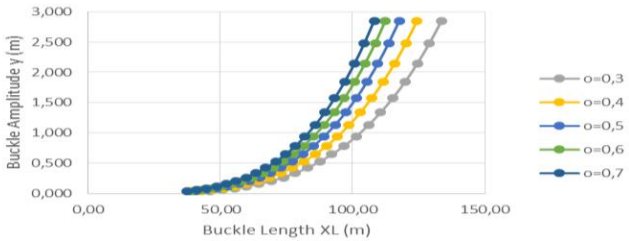

Figure 16. Graph correlation of buckling length (L) to the buckling amplitude (y) mode 1.

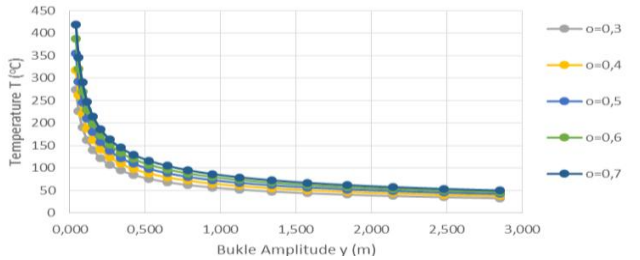

Figure 17. Graph correlation of buckling length (L) to temperature changed (T) mode 1.

For the chart of 2-4 modes has a pattern identical or similar to the mode 1 because the coefficient which are used is not too different.

4.4 Comparison of the Analysis Result between Vertical Buckling and Lateral Buckling

The comparisons are made between the vertical buckling the actual coefficient with lateral buckling mode 1, because both modes have in common is the concept.

On the lateral buckling, the buckling length increases, from the extremely high temperatures fell significantly by buckling length (L) to 10 and then the temperature (T) to increase slowly. Unlike the lateral buckling mode 1. The buckling length (L), then the temperature (T) decrease of temperature (T) is very high. This occurs due to the influence of axial stress (P_0) are different between the vertical buckling by lateral buckling in which the required vertical buckling axial stress (P_0) is greater than on the lateral buckling.

For a comparison between buckling length (L) with the buckling amplitude (y) looks almost the same pattern: the longer owned buckling (L) happens, the higher the amplitude (y) buckling occurring. However, there is little difference that the vertical buckling curve, the coefficient of friction does not affect the relationship between the buckling length (L) with the buckling amplitude (y). While in lateral buckling mode 1, the higher the coefficient of friction on buckling amplitude (y) of the same, then the buckling length (L) will decrease. This is because the coefficient of friction on the lateral buckling is assumed to be at each end of the surface.

4.5 Vertical Buckling Analysis Using DNV RP F110

Axial stress analysis (S_{eff}) performed in the range of coefficients of friction of $0.3 \leq \varphi \leq 0.7$. Using the equation 17, then obtained axial stress (S_{eff}) as follows:

Table 3.The value of effective axial stress (S_{eff}) on the vertical buckling.

No.	Friction Coefficient	S eff atau P_0 (Pa)
1	0,03	9643960,454
2	0,04	9643983,556
3	0,05	9644006,658
4	0,06	9644029,760
5	0,07	9644052,861

Based on the table above, the higher of the friction coefficient can be results in the higher of axial stress (S_{eff}).

4.6 Lateral Buckling Analysis Using DNV RP F110

Just as before, the analysis was done on a friction coefficient of $0.3 \leq \varphi \leq 0.7$ and the range of variation in the length of buckling as many as 20 (with a value range 0,1L-3L). L_{min} then obtained as follows:

Table 4. The minimum buckling length (L) for lateral buckling.

No.	Friction Coefficient	Buckling Length L (m)
1	0,30	157,40
2	0,40	146,48
3	0,50	138,53
4	0,60	132,36
5	0,70	127,35

Using a length of buckling above, is obtained the following graph,,

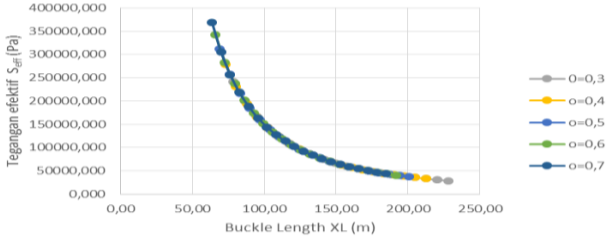

Figure 18. Graph correlation of buckling length (L) to the effective stress by DNV RP F110.

Based on the table, a decline in the effective axial stress ($S\infty$) from the initially very high and then descend slowly along with the growing length of buckling occurred.

4.7 The Comparation of Axial Hobbs Stress to DNV RP F110

For vertical buckling use DnV RP F110, axial stress (S_{eff}) is not influenced by the length of buckling. So that the same coefficient, axial stress (S_{eff}) happens to be constant, but will be increased with the increase in the coefficient of friction (φ). Instead, Hobbs method using buckling length (L) into one of the variables. So any changes will affect the long-buckling axial stress (P_0) experienced pipe buckling to occur.

As for lateral buckling use DnV RP F110 is not explained in detail every buckling mode that occurs as the method of Hobbs. But the same pattern occurred between the results of the method Hobbs mode DnV 1-4 with the results of RP F110.

Based on the table explained that both originated from axial high stress, then moved down along with the increase in length of buckling (xL) happens. But it is different with the results Hobbs method for lateral buckling infinite mode. In this mode, the voltage axial (P_0) move down from the initially very high, then increases again in the 12^{th} variation.

5. CONCLUSIONS

Based on the analysis and discussion process that has been done, a few of conclusions as follows:

1. The correlation between the coefficient of friction to buckling length (L), the amplitude of buckling (Y) and temperature (T)
   a. Vertical buckling: The greater the coefficient of friction (φ), then the temperature (T) increased to 12.95%. In contrast, the coefficient of friction does not affect the buckling length (L) and buckling amplitude (y)
   b. Lateral buckling: The greater the coefficient of friction (φ), the buckling length (L) will be reduced to 6.94%, the temperature (T) increased to 13.4%, but did not affect the amplitude of buckling (y).
2. Comparison between the vertical lateral buckling include:
   a. In the vertical buckling curve, the coefficient of friction does not affect, while the lateral buckling mode 1, the higher the coefficient of friction on the amplitude of buckling (y) is the same, then the buckling length (L) decreases to 6.94%.
   b. On the lateral buckling, the increasing length of buckling, high temperature fell significantly by buckling length (L) to 10 and then the temperature (T) increased to 12.95%. While lateral buckling mode 1, the buckling length (L), then the temperature (T) will fall to 13.4%.
3. The comparison of Hobbs method and DNV RP F110
   a. Vertical Buckling
      In DnV RP F110, the higher the coefficient of friction, the axial stress (S_{eff}) increased by 0.00024%. In contrast to the method of Hobbs, axial stress (P0) decreased and increased to 12.95%.
   b. Lateral Buckling
      In the method of Hobbs mode 1-4 and DnV RP F110 have the same pattern that begins with high axial tension, then descends with the increase in long-buckling (xL). But for lateral buckling infinite mode in Hobbs where axial stress (P0) getting down from the initially very high, then climbed back on the variation to the 12th with a percentage decrease or increase up to 13.4%.

ACKNOWLEDGEMENTS

The author would like to thank all those who have supported and helped make this research can be done well.

REFERENCES

1. DNV OS F101: *Submarine Pipeline System*. Det Norske Veritas. Norwey. 2007.
2. DNV RP F109: *On Bottom Stability Design of Submarine Pipelines*. Det Norske Veritas. Norwey. 2010.
3. DNV RP F110: *Global Buckling of* Submarine *Pipelines, Structural Design due to High Temperature/High Pressure.* Det Norske Veritas. Norwey. 2007.
4. DNV RP F109: *On Bottom Stability Design of Submarine Pipelines*. Det Norske Veritas. Norwey. 2010.
5. Febrian, Dian: *Perbandingan Analisa Free Span Menggunakan DNV RP F-105 "Freespanning Pipeline" dengan DNV 1981 "Rule for Submarine Pipelines System"*. Tugas Akhir, Jurusan Teknik Kelautan-FTK, Institut Teknologi Sepuluh Nopember, Surabaya. 2013.
6. Hobbs, R. E: *Pipeline Buckling Caused by Axial Loads*. Jurnal. Journal of Constructional Steel Research: Vol. 1, No. 2. London. 1981.
7. Irawan, D.: *Studi Kuat Tekan Kolom Baja Profil C dengan Perkuatan Tulangan Tranversal dan Cover Plate.* Tugas Akhir, Universitas Atma Jaya, Yogyakarta. 2014.
8. Popov, E. P.: *Mekanika Teknik (Mechanics of Materials)*. Erlangga. Jakarta. 1989
9. Prayoga, Friga Surya: *Studi Pengaruh Temperatur, Tekanan Internal, dan Kedalaman Tanah terhadap Mekanisme Upheaval Buckling pada Onshore Pipeline.* Tugas Akhir, Jurusan Teknik Kelautan-FTK,

Institut Teknologi Sepuluh Nopember, Surabaya. 2011.

10. Shi, Ruowei, Wang, Kuanjun, Long, Fan. dan Li, Hongwei: *Vertical Buckling of Offshore Pipelines with Geometrical Imperfection on Soft Seabed.* Jurnal. EJGE, Vol. 18. China. 2013.
11. Soegiono: *Pipa Bawah Laut*. Surabaya: Airlangga University Press. 2007.
12. Wright, Douglas: *Notes on: Design and Analysis of Machine Elements*. Department of Mechanical and Materials Engineering, The University of Western Australia. Perth. 2005.
13. Xiaodi, Song, dan Xiaoxian, Song: *Study of Lateral* Buckling *of Submarine Pipeline.* Jurnal. 2nd International Conference on Electronic & Mechanical Engineering and Information Technology (EMEIT). China. 2012.